UCSF

UC San Francisco Previously Published Works

Authors

Odegaard, Justin I
Lee, Min-Woo
Sogawa, Yoshitaka
et al.

Perinatal licensing of thermogenesis by IL-33 and ST2

Justin I. Odegaard[#,1], **Min-Woo Lee**[#,1], **Yoshitaka Sogawa**[#,1], **Ambre M. Bertholet**[2], **Richard M. Locksley**[3,4,5], **David E. Weinberg**[6], **Yuriy Kirichok**[2], **Rahul C. Deo**[1,3], and **Ajay Chawla**[1,2,3]

[1]Cardiovascular Research Institute, University of California, San Francisco, 94143-0795, USA

[2]Department of Physiology, University of California, San Francisco, 94143-0795, USA

[3]Department of Medicine, University of California, San Francisco, 94143-0795, USA

[4]Department of Microbiology & Immunology, University of California, San Francisco, 94143-0795, USA

[5]Howard Hughes Medical Institute, University of California, San Francisco, 94143-0795, USA

[6]Department of Cellular and Molecular Pharmacology, University of California, San Francisco, 94143-0795, USA

[#] These authors contributed equally to this work.

SUMMARY

For placental mammals, the transition from the in utero maternal environment to postnatal life requires the activation of thermogenesis to maintain their core temperature. This is primarily accomplished by induction of uncoupling protein 1 (UCP1) in brown and beige adipocytes, the principal sites for uncoupled respiration. Despite its importance, how placental mammals license their thermogenic adipocytes to participate in postnatal uncoupled respiration is not known. Here, we provide evidence that the 'alarmin' IL-33, a nuclear cytokine that activates type 2 immune responses, licenses brown and beige adipocytes for uncoupled respiration. We find that, in absence of IL-33 or ST2, beige and brown adipocytes develop normally but fail to express an appropriately spliced form of *Ucp1* mRNA, resulting in absence of UCP1 protein, and impairment in uncoupled respiration and thermoregulation. Together, these data suggest that IL-33 and ST2 function as a developmental switch to license thermogenesis during the perinatal period.

Graphical abstract

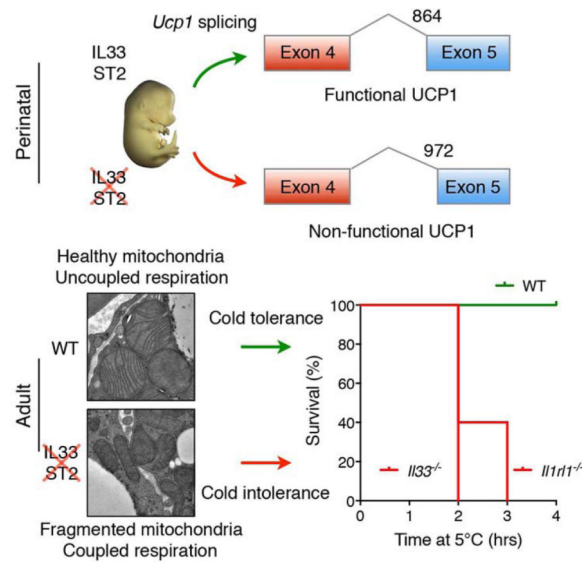Correspondence: ajay.chawla@ucsf.edu.

eTOC

A signal from the immune system mediates the activation of thermogenesis during the transition from the in utero maternal environment to postnatal life, allowing animals to maintain their core temperature in cold environments.

INTRODUCTION

The maintenance of core temperature is essential to ensure that cellular and physiological functions operate normally in endotherms under conditions of environmental challenge (Cannon and Nedergaard, 2011; Gordon, 1993). In mammals, two types of programs support thermal homeostasis in cold environments: heat conservation and heat generation (Cannon and Nedergaard, 2011; Lowell and Spiegelman, 2000). While vasoconstriction and piloerection are the major means of conserving heat, shivering and adaptive thermogenesis are the principal mechanisms by which mammals increase heat production in order to adapt and acclimatize to colder environments. In support of this, genetic mutations in mice that disrupt cellular programs of adaptive thermogenesis impair thermoregulation and reduce organismal fitness in the cold (Bachman et al., 2002; Enerback et al., 1997).

Brown and beige adipocytes are the major cellular sites for heat production in mammals (Cohen and Spiegelman, 2015; Harms and Seale, 2013; Vosselman et al., 2013). In both of these thermogenic tissues, uncoupling protein 1 (UCP1), which resides in the inner mitochondrial membrane, uncouples oxidative phosphorylation (OXPHOS) from ATP synthesis to stimulate metabolic respiration and heat generation. Although a number of other uncoupling proteins have been identified in mammals and non-mammalian species (Azzu and Brand, 2010), only UCP1 has been shown to function as an "uncoupler" by conducting protons across the inner mitochondrial membrane (Fedorenko et al., 2012; Klingenberg et al., 1999). In line with this, mice lacking *Ucp1* are unable to increase metabolic respiration upon cold exposure and rapidly succumb to hypothermia (Enerback et al., 1997). Since UCP1 also participates in diet-induced thermogenesis to regulate energy balance and body

weight (Bachman et al., 2002; Feldmann et al., 2009), there is great clinical interest in identifying pathways that induce or maintain expression of UCP1 in thermogenic adipocytes for the treatment of human obesity (Harms and Seale, 2013).

Prolonged exposure to environmental cold results in recruitment of beige and brown adipocytes in mice and humans to increase total thermogenic capacity (Frontini and Cinti, 2010; Harms and Seale, 2013; Sidossis and Kajimura, 2015). Whilst this cold-induced increase in brown adipose tissue (BAT) mass is driven by its adrenergic activation by the sympathetic nervous system (Cannon and Nedergaard, 2011; Lowell and Spiegelman, 2000), recruitment of thermogenic beige adipocytes also relies on signals from the innate immune system. For example, we and others have found that cold- and myokine-induced biogenesis of beige fat requires type 2 innate immune cells and signals, including eosinophils, alternatively activated macrophages, and the type 2 cytokines interleukin–4 and –13 (IL-4 and –13) (Lee et al., 2015; Nguyen et al., 2013; Qiu et al., 2014; Rao et al., 2014). Since group 2 innate lymphoid cells (ILC2s) are the major innate source of IL-13 and IL-5 (the latter being required for the survival and proliferation of eosinophils) (Moro et al., 2010; Neill et al., 2010; Nussbaum et al., 2013; Price et al., 2010), gain-of-function approaches have implicated ILC2s and IL-33, an activator of ILC2s, in the biogenesis of thermogenic beige fat (Brestoff et al., 2015; Lee et al., 2015). For instance, we found that administration of IL-33 to thermoneutral adult mice resulted in the activation of ILC2s and recruitment of beige fat in an IL-4Rα-dependent manner (Lee et al., 2015). In a similar manner, Brestoff et. al. reported that treatment of adult mice, which were housed at the normal vivarium temperature, with IL-33 stimulated the recruitment of beige adipocytes in an ILC2-dependent manner (Brestoff et al., 2015). While these gain-of-function studies implicated IL-33 and ILC2s in biogenesis of beige adipose tissue, it is not known whether ILC2s or IL-33 are physiologically required for development of functional beige or brown adipocytes and for adaptation to environmental cold.

IL-33, a member of the IL-1 family, is a type 2 cytokine that is constitutively expressed in the nucleus of epithelial cells, endothelial cells, and fibroblasts (Pichery et al., 2012). A number of factors have been identified that trigger the release of IL-33 from cells, including infectious agents, allergens, necrotic cell death, and mechanical stretch (Cayrol and Girard, 2014; Molofsky et al., 2015). Based on the observation that IL-33 is stored in the nucleus as a pre-formed cytokine and released by cellular stress, it has been suggested that IL-33 acts as an 'alarmin' to alert the immune system of potential tissue stress or damage (Cayrol and Girard, 2014; Molofsky et al., 2015). In this context, the released and cleaved forms of IL-33 activate immune cells expressing ST2, such as ILC2s and regulatory T cells (Tregs), to initiate downstream effector responses (Bapat et al., 2015; Kolodin et al., 2015; Molofsky et al., 2013; Vasanthakumar et al., 2015).

Here, we address the requirement of IL-33:ST2 axis on the physiologic development of beige and brown adipocytes. We report that, unlike the type 2 cytokines IL-4 and –13, IL-33:ST2 and ILC2s are not required for the commitment or differentiation of beige adipocytes. Rather, we find that IL-33:ST2 act in a non-canonical manner to perinatally license uncoupled respiration in thermogenic adipocytes. The term 'license' is used here to denote a switch from a previous default state to a new permissive state. For example, in

brown adipocytes, this represents a permanent switch from 'coupled' respiration in the embryo to 'uncoupled' respiration in the neonate. Our findings thus uncover an unexpected mechanism by which IL-33:ST2 function as a developmental switch to license BAT for its postnatal functions in thermogenesis.

RESULTS

IL-33 is required for uncoupled respiration in beige adipocytes

To investigate the requirement of IL-33 in cold-induced beige fat development, we challenged 8-week-old C57BL/6J (WT) and congenic *Il33*^{−/−} mice with exposure to environmental cold (5°C) for 48 hours. As assessed by expression of UCP1 protein, WT mice exhibited robust browning of their inguinal WAT (iWAT), a metabolic adaptation that was absent in *Il33*^{−/−} mice (Figure 1A). *Ex vivo* analysis of oxygen consumption verified that exposure to environmental cold increased thermogenic capacity of iWAT in an IL-33-dependent manner (Figure 1B). Although immunoreactive UCP1 protein was absent in representative tissue sections of *Il33*^{−/−} mice (Figure 1C), hematoxylin and eosin staining revealed the presence of more beige and fewer white adipocytes in iWAT of *Il33*^{−/−} mice (Figure 1D). In aggregate, these findings suggest that IL-33 is not required for the commitment to the beige adipocyte lineage but rather for licensing its functions in uncoupled respiration.

In mice, physiologic recruitment of beige fat occurs at time of weaning (Lee et al., 2015; Xue et al., 2007), prompting us to ask whether IL-33 is also required for this metabolic remodeling of iWAT. Immunoblotting for UCP1 revealed that its expression peaked at postnatal day 21 (P21) in iWAT of WT mice followed by a gradual decline as mice aged (Figure 1E). This physiological uncoupling of metabolic respiration was absent in iWAT of *Il33*^{−/−} mice (Figure 1E). Moreover, hematoxylin and eosin staining revealed the presence of multilocular beige adipocytes in *Il33*^{−/−} mice as early as P7 that persisted through adulthood (Figure S1A). While this recruited beige adipose tissue in *Il33*^{−/−} mice did not express UCP1 protein (Figure 1E), it had higher expression of thermogenic genes and mitochondrial content (Figure S1B-E), potentially pointing to a compensatory response for thermogenic defects in other fat depots. In line with this, similar histological changes and an increase in oxidative metabolism were observed in iWAT of *Ucp1*^{−/−} mice, which were housed at 20°C or gradually acclimated to 4°C (Liu et al., 2003; Ukropec et al., 2006).

To understand the underlying mechanisms for these observations, we performed whole-genome gene expression analysis (RNA-seq) on iWAT isolated from WT and *Il33*^{−/−} mice at P24, a time point corresponding to physiologic browning of iWAT. After normalization of datasets, we used FuncAssociate to identify pathways that were induced or repressed (FDR<5% and >2-fold expression) in iWAT of *Il33*^{−/−} mice (Berriz et al., 2003). Consistent with histological presence of multilocular beige adipocytes in *Il33*^{−/−} mice (Figure S1A), we found that the expression of beige fat markers was not significantly different amongst the genotypes (Figure 1F). While gene ontologies associated with skeletal muscle contraction, antiviral immunity, and angiogenesis were repressed in iWAT of *Il33*^{−/−} mice (Figure 1G and Table S1, S3), gene ontologies associated with catabolism of fatty acids, glucose, and branched chain amino acids were all induced in *Il33*^{−/−} mice (Figure 1H and Table S2, S3).

These data suggest that $Il33^{-/-}$ mice compensate for defects in uncoupled respiration by increasing flux through various catabolic pathways. Since Spiegelman and colleagues recently identified creatine-driven substrate cycle as a potential means of generating heat in the absence of UCP1 (Kazak et al., 2015), we examined the expression of genes involved in the creatine-driven substrate cycle in our RNA-seq datasets. While expression of $Ckmt1$ and $Slc6a8$ was unchanged, expression of $Ckmt2$, $Gatm$, and $Gamt$ was reduced by ~2-4-fold in iWAT of $Il33^{-/-}$ mice (Tables S3), suggesting that the creatine-driven substrate cycle is unlikely to compensate for thermogenic defects in iWAT of $Il33^{-/-}$ mice.

Defective cold-induced thermogenesis in $Il33^{-/-}$ mice

During the course of these studies, we noticed that a subset of $Il33^{-/-}$ mice were not able to maintain their core temperature after exposure to environmental cold (Figure S1F). This impairment in thermoregulation compromised the survival of 8.5-week-old $Il33^{-/-}$ mice when they were housed at 4°C (Figure 2A). Upon exposure to environmental cold, mice activate preformed thermoeffectors, such as shivering and brown adipose tissue (BAT), to generate heat (Cannon and Nedergaard, 2011; Gordon, 1993; Lowell and Spiegelman, 2000). To address whether IL-33 deficiency affects shivering or nonshivering thermogenesis, we challenged young mice, which have smaller muscle mass and lower capacity to generate heat by shivering, with environmental cold. We found that 4.5- and 5.5-week-old $Il33^{-/-}$ mice exhibited a more profound decrease in their rate of survival during a cold challenge at 4°C (Figure 2B and S1G). These observations are in line with what has been previously reported for $Ucp1^{-/-}$ mice, which lack non-shivering thermogenesis. In this case, the penetrance of cold sensitivity was found to be dependent on the genetic background of $Ucp1^{-/-}$ mice and the life history of acclimation to environmental cold (Golozoubova et al., 2001; Hofmann et al., 2001).

To investigate a potential defect in nonshivering thermogenesis in $Il33^{-/-}$ mice, we measured oxygen consumption in WT and $Il33^{-/-}$ mice after administration of norepinephrine, which activates thermogenic and metabolic programs without inducing shivering (Cannon and Nedergaard, 2011). We found that oxygen consumption rate was reduced by ~25% in $Il33^{-/-}$ mice (Figure 2C, D), pointing to a primary defect in brown fat thermogenesis. Congruent with these data, gross and microscopic histology revealed that the interscapular brown adipose tissue (BAT) of $Il33^{-/-}$ mice was paler, larger (~2-fold), and contained more lipid droplets (Figure 2E, F and Figure S1H). Taken together, these data suggest that a defect in brown fat thermogenesis in $Il33^{-/-}$ mice compromises their survival in the cold, thereby providing an explanation for increased recruitment of beige-like adipocytes in iWAT.

To gain molecular insights into how IL-33 deficiency affects BAT thermogenic programs, we performed RNA-seq analysis on BAT isolated from WT and $Il33^{-/-}$ mice at P0.5. We chose this early time point to limit the secondary effects of prolonged cold stress that results from housing mice at 22°C, a temperature that is well below their thermoneutral zone (Cannon and Nedergaard, 2011; Gordon, 1993), and has dramatic effects on their immune and metabolic programs (Karp, 2012; Tian et al., 2016). Congruent with the histological presence of BAT in $Il33^{-/-}$ mice, genetic deficiency of IL-33 did not significantly alter expression of brown fat identity genes, such as $Ucp1$, $Dio2$, $Prdm16$, and $Ppargc1a$ (Figure

2G, Table S5). Gene term enrichment analyses revealed that no specific gene ontologies were suppressed in BAT of *Il33*^{−/−} mice, whereas an immediate early-gene stress signature (including *Fos*, *Jun*, *Atf3*, *Cebpd*, *Fosl2*, *Junb*, *Nfkbia*, and *Phdla3*) heavily dominated the gene ontologies that were induced in *Il33*^{−/−} mice (Figure 2H and Table S4, S5), potentially suggesting that impairment in thermogenic function results in metabolic and oxidative stress in BAT of *Il33*^{−/−} mice.

IL-33 is required for splicing of Ucp1 mRNA and expression of functional UCP1

Brown adipose tissue is the primary site of uncoupled respiration in mice. To investigate the mechanisms by which IL-33 regulates BAT functionality, we first quantified oxygen consumption by BAT *ex vivo*. Compared to WT mice, the rate of oxygen consumption was reduced by ~75% in BAT of *Il33*^{−/−} mice (Figure 3A and Figure S2A). As assessed by immunoblotting and immunohistochemistry, this decrease in oxygen consumption likely resulted from the absence of UCP1 protein in BAT of *Il33*^{−/−} mice that were housed at 22°C or 5°C (Figure 3B, C). Of note, the analyses at 5°C were performed with tissues obtained from *Il33*^{−/−} mice that survived the acute cold challenge (Figure 2A and Figure S1B). This defect in UCP1 protein expression likely reflects a developmental failure in licensing of uncoupled respiration in BAT, because it was present in *Il33*^{−/−} BAT at P0.5 and persisted through adulthood (Figure S2B-G). Congruent with this, administration of IL-33 or the β3-adrenergic agonist CL 316,243 failed to restore UCP1 protein expression in adult (8-10 week-old) *Il33*^{−/−} mice (Figure S2H). Furthermore, cohousing of *Il33*^{−/−} with WT neonatal pups did not rescue UCP1 protein expression in BAT, suggesting that changes in the microbiome are unlikely to account for these differences in uncoupled respiration between the two genotypes (Figure S2I).

Although UCP1 protein was absent in the BAT of *Il33*^{−/−} mice, we found that *Ucp1* mRNA was expressed in IL-33-deficient BAT, albeit its expression was reduced by ~2-fold (Figure 2G). These observations suggested that impaired translation or alternative splicing might interfere with the detection of UCP1 protein by immunoblotting. To distinguish between these two possibilities, we assessed the translation of *Ucp1* mRNA by isolating polysomes from BAT. We found that similar amounts of *Ucp1* mRNA were present in the polysome fractions isolated from BAT of WT and *Il33*^{−/−} mice (Figure 3D), indicating that impairment in translation is less likely to account for the absence of UCP1 protein in *Il33*^{−/−} mice.

We next asked whether alternative splicing of *Ucp1* mRNA might account for the absence of UCP1 protein in BAT of *Il33*^{−/−} mice. Analysis of RNA-seq datasets revealed the activation of alternative splice sites in exon 5 of *Ucp1* gene in BAT of *Il33*^{−/−} mice. For example, while majority of the *Ucp1* mRNAs in BAT of WT mice utilized the normal splice junctions between exon 4 and 5 (splice variant A), *Ucp1* mRNAs present in *Il33*^{−/−} BAT had an alternative splicing pattern (Figure 3E, F). In BAT of *Il33*^{−/−} mice, we found activation of cryptic acceptor splice sites in exon 5 that resulted in generation of two alternatively spliced variants (B and C) of *Ucp1* mRNA (Figure 3E). Quantification of splice junction reads revealed that ~85% of *Ucp1* mRNAs encoded for splice variants B (~15%) and C (~70%) in *Il33*^{−/−} mice, whereas ~98% of the junction reads encoded for the normal splice variant A in BAT of WT mice (Figure 3F). Furthermore, we found a similar distribution of *Ucp1* mRNA

splice variants in iWAT of $Il33^{-/-}$ mice (Figure S3A). Since ~9% of the junction reads encoded for splice variant C in one of WT BAT samples (Figure 3F), we wondered whether it was normally present in BAT of WT mice. To address this question, we designed primers that specifically amplified splice variants A and C, and used them to quantify its abundance in BAT. Quantitative RT-PCR analysis revealed that mRNAs encoding for splice variant C were readily detectable and had a similar temporal pattern of expression as the normal splice variant A in embryonic and adult BAT of WT mice (Figure S3B, C). Together, these findings suggest that at least two splice variants of $Ucp1$ mRNA (A and C) are normally expressed in BAT of WT mice, and IL-33 functions as a developmental switch to suppress the expression of variant C and increase expression of variant A in thermogenic adipocytes.

Since these alternative spliced forms resulted in in-frame deletions in UCP1 protein (variant B has a 9 amino acid deletion, whereas variant C has a 36 amino acid deletion), they are likely to escape nonsense-mediated mRNA decay and be translated, as suggested by the presence of $Ucp1$ mRNAs in the polysomes of $Il33^{-/-}$ BAT (Figure 3D). However, it is unclear whether proteins translated from these alternatively spliced $Ucp1$ mRNAs will be stable, because both predicted proteins will lack part of or the entire region encompassing the 5th transmembrane segment of UCP1, which is required for its insertion into the inner mitochondrial membrane (Klingenberg et al., 1999). We thus asked whether protein products encoded from these alternatively spliced variants were present in P0.5 BAT. By immunoblotting for UCP1, we detected a faint band that was ~1kDa smaller than the full length UCP1 in BAT of $Il33^{-/-}$ mice. Since this band was absent in BAT of WT or $Ucp1^{-/-}$ mice, it suggests that it is likely encoded from $Ucp1$ splice variant B, which is only present in BAT of $Il33^{-/-}$ mice (Figure 3F, G). The predicted size of protein encoded by splice variant C is ~4kDa smaller, which would be expected to migrate around the non-specific ~25kDa band that is found in all three genotypes (Figure 3G). Thus, we employed an orthogonal approach to determine whether these alternative splice variants can encode for a functional UCP1 protein. For this, we measured UCP1-mediated proton conductance in mitoplasts isolated from BAT of WT and of $Il33^{-/-}$ mice. While the characteristic guanosine diphosphate (GDP)-inhibitable UCP1 proton current was detected in WT mitoplasts (Fedorenko et al., 2012), it was absent in mitoplasts prepared from BAT of $Il33^{-/-}$ mice (Figure 3H, I), indicating that UCP1 mRNAs expressed in BAT of $Il33^{-/-}$ mice do not encode for a functional UCP1 protein.

ST2 is required for uncoupled respiration in thermogenic adipocytes

IL-33 binds to and signals via the ST2 receptor (encoded by $Il1rl1$) (Schmitz et al., 2005), prompting us to ask whether $Il1rl1$ is similarly required for uncoupled respiration in beige and brown adipocytes. Immunoblotting revealed robust expression of UCP1 protein in iWAT of 4-week-old WT mice, which corresponded to the physiologic browning of this tissue (Figure 4A). In contrast, iWAT of congenic $Il1rl1^{-/-}$ mice failed to express UCP1 protein (Figure 4A). A similar requirement for ST2 was observed in BAT, which grossly and histologically resembled BAT of $Il33^{-/-}$ mice, as it was paler, larger, and contained more cytoplasmic lipid droplets (Figure 4B, C, Figure 2E, and Figure S1D). Furthermore, BAT of $Il1rl1^{-/-}$ mice lacked UCP1 protein and UCP1-mediated proton current (Figure 4D-F), and expressed the alternative (C) but not the normal (A) variant for $Ucp1$ mRNA (Figure S3D,

E). As a consequence, 4.5-week-old *Il1rl1*^{−/−} mice failed to survive an acute cold challenge (Figure 4G), because they were unable to maintain their core temperature (Figure 4H). Together, these results establish epistasis between IL-33 and ST2, and suggest that IL-33:ST2 function as a developmental switch to regulate uncoupling capacity of beige and brown adipocytes.

Previous gain-of-function studies demonstrated that IL-33 activates ILC2s, a ST2 expressing cell that is the major cellular source of type 2 cytokines, to recruit beige adipose tissue (Brestoff et al., 2015; Lee et al., 2015). However, our current studies with IL-33 and ST2 null mice suggest that IL-33:ST2 and IL4/13:IL-4Rα have distinct requirements in recruitment of thermogenic adipocytes. First, while IL-4/13:IL-4Rα signaling is required for the commitment and maturation of beige adipocytes (Lee et al., 2015; Qiu et al., 2014), IL-33 and ST2 are only required for the expression of UCP1 protein in beige adipocytes. Second, unlike the specific requirement for IL-4/13 signaling in beige adipogenesis, IL-33 and ST2 are required for uncoupling of metabolic respiration in both beige and brown adipocytes. These differences between the requirements of IL-33 and IL4/13 in thermogenesis led us to ask whether ILC2s are the critical target by which IL-33 and ST2 license uncoupled respiration. To test this hypothesis, we utilized RRDD mice in which all IL-5-expressing cells, such as ILC2s and Th2 cells, are deleted by Cre recombinase-mediated expression of diphtheria toxin A (Van Dyken et al., 2014). As expected, ILC2s and IL-5-expressing cells were absent in BAT, iWAT, and epididymal WAT of RRDD mice (Figure S4A-C). However, unlike IL-33 or ST2 deficiency, loss of ILC2s did not affect uncoupled respiration in brown or beige adipocytes. For example, we found no differences in BAT UCP1 protein expression, oxygen consumption, or cellular histology between WT and congenic RRDD mice (Figure S4D-F). In a similar manner, we observed that cold-induced and physiologic browning of iWAT was intact in RRDD mice (Figure S4G, H). Analysis of Rag2^{−/−}/γc^{−/−} mice revealed a similar lack of requirement for adaptive immune cells, including Tregs and ILCs, in uncoupling of metabolic respiration in brown adipocytes (Figure S4I).

In immune cells, the adaptor protein MyD88 confers responsiveness to IL-33 (Molofsky et al., 2015), leading us to ask whether MyD88 was also required for uncoupled respiration. In contrast to our results with mice deficient in *Il33* or *Il1rl1*, we found that *MyD88* was dispensable for UCP1 protein expression in brown and beige adipocytes (Figure 4I and Figure S4J). These findings together suggest that IL-33:ST2 likely utilize a non-canonical pathway to developmentally license uncoupled respiration in thermogenic adipocytes.

Reduced oxidative respiration and complex activity in mitochondria of IL-33 deficient BAT

Since BAT of *Il33*^{−/−} and *Il1rl1*^{−/−} mice lacked the mitochondrial protein UCP1, we asked whether loss of IL-33 or ST2 also affected mitochondrial respiration and complex activity. To this end, we purified mitochondria from BAT WT and *Il33*^{−/−} mice, and used western blotting to assess their purity. Although total mitochondrial content and protein were increased in *Il33*^{−/−} mice (Figure S5A, B), this largely reflected an increase in their BAT mass (Figure 2F and S5C). Immunoblotting with the purified mitochondria revealed

enrichment of mitochondrial proteins along with efficient removal of contaminating cytosolic proteins (Figure S5D).

Using purified mitochondrial preparations from ~6-week-old mice, we quantified mitochondrial respiration via a Clarke-type electrode in the presence of substrates and mitochondrial inhibitors (Figure 5A, B). As expected, oxygen consumption rate increased in WT mitochondria after the addition of the substrate palmitoyl-coenzyme A. This substrate-induced increase in oxidative respiration, which was inhibited by the addition of GDP, was lower in mitochondria isolated from *Il33*$^{-/-}$ BAT, findings that are consistent with the lack of functional UCP1 in BAT of these animals. In contrast to WT mitochondria, ADP-stimulated coupled respiration was higher in mitochondria of *Il33*$^{-/-}$ BAT (Figure 5A, B). However, despite this increase in coupled respiration, the maximal oxidative capacity, which was measured in the presence of the uncoupler carbonyl cyanide- p-trifluoromethoxyphenylhydrazone (FCCP), was reduced in mitochondria purified from *Il33*$^{-/-}$ BAT (Figure 5A, B).

Based on these findings, we asked whether changes in the mitochondrial complexes contribute to the decrease in mitochondrial oxidative capacity observed in *Il33*$^{-/-}$ BAT. To address this question, we quantified the expression and activity of respiratory chain components in purified mitochondria. Immunoblotting revealed reduction in expression of complex I (NDUFB8) and IV (MTCO1) components in mitochondria of *Il33*$^{-/-}$ BAT (Figure 5C). This was accompanied by increased expression of complex V protein ATP5A, cytochrome C, and VDAC1 in mitochondria of *Il33*$^{-/-}$ BAT (Figure 5C). Quantification of respiratory complex activities affirmed that activities of complex I and IV were reduced by ~68% and ~46%, respectively (Figure 5D, G), whereas those of complex II and III were not significantly different between the genotypes (Figure 5E, F). These changes in OXPHOS protein expression were specific for BAT because we failed to detect similar changes in the expression of mitochondrial respiratory components in hearts of *Il33*$^{-/-}$ mice (Figure S5E), a tissue that is highly oxidative and previously shown to be responsive to IL-33 (Chen et al., 2015).

The observed alterations in OXPHOS and respiratory activity prompted us to ask whether loss of IL-33 resulted in ultrastructural changes in the mitochondria of *Il33*$^{-/-}$ BAT. Compared to WT mitochondria, transmission electron microscopy demonstrated that mitochondria of *Il33*$^{-/-}$ BAT were smaller and irregularly shaped, and their cristae were malformed and present at a lower density (Figure 5H, I). Exposure to environmental cold exacerbated these ultrastructural defects in BAT of *Il33*$^{-/-}$ mice, as evidenced by the paucity of normal cristae, reduced mitochondrial size, and presence of mitochondrial inclusions (Figure 5J, K). In aggregate, these findings potentially suggest a much broader role for IL-33 in the regulation of mitochondrial assembly and respiration.

Mitochondria of *Ucp1*$^{-/-}$ BAT have defects in respiratory complexes

Although mitochondria from BAT of adult *Il33*$^{-/-}$ mice exhibit profound structural and respiratory defects, our RNA-seq experiments using P0.5 BAT failed to detect significant changes in the expression of mitochondrial genes (Figure 2 and Tables S4, S5). A potential answer to this paradox might be that the failure to express a functional UCP1 protein is the

primary defect in BAT of $Il33^{-/-}$ mice, which later translates into the observed mitochondrial dysfunction as animals age. We thus reasoned that quantitative analysis of mitochondrial complex activity in $Ucp1^{-/-}$ mice, which only harbor mutation in the $Ucp1$ gene, might provide an unequivocal test of this hypothesis. Similar to $Il33^{-/-}$ mice, we found that BAT mitochondria of ~6-week-old $Ucp1^{-/-}$ mice had reduced expression of complex I (NDUFB8) and IV (MTCO1) components, whereas expression of components of complex II, III, and V was unaltered (Figure 6A). Unlike $Il33^{-/-}$ mice, however, we failed to detect compensatory increase in cytochrome C (CytC), which is necessary for electron transfer between respiratory complexes III and IV. These changes were specific to BAT because expression of respiratory chain components was unaltered in hearts of these animals (Figure 6B).

We next asked whether BAT of $Ucp1^{-/-}$ mice had similar respiratory and structural defects as those observed in $Il33^{-/-}$ mice. We found that the respiratory activities of complex I and IV were reduced by ~75% and ~85%, respectively (Figure 6C, D). Ultrastructural analysis of BAT of $Ucp1^{-/-}$ mice showed similar defects in their mitochondria as were observed in BAT of $Il33^{-/-}$ mice. For example, we observed that $Ucp1^{-/-}$ mitochondria were smaller, varied in size and shape, and had lower cristae density that were irregular and malformed (Figure 6E, F). These functional and structural similarities in mitochondria of $Ucp1^{-/-}$ and $Il33^{-/-}$ mice suggest that deficiency of UCP1 likely contributes to the mitochondrial dysfunction observed in BAT of $Il33^{-/-}$ mice.

Perinatal requirement of IL-33 and ST2 in licensing of uncoupled respiration

Our cumulative data suggest that a primary defect in UCP1 protein expression, such as in $Il33^{-/-}$ or $Ucp1^{-/-}$ mice, alters mitochondrial respiration, which later manifests as mitochondrial dysfunction in older animals. If this is correct, then the mitochondrial defects observed in BAT of $Il33^{-/-}$ or $Ucp1^{-/-}$ mice should be absent in younger animals. To test this hypothesis, we analyzed expression of UCP1 protein in BAT during embryonic development and the perinatal period. We found that BAT of WT mice gains competence for uncoupled respiration at embryonic day (E18.5), one day prior to birth, which occurred at P0.5 in this series of timed matings (Figure 7A). In $Il33^{-/-}$ mice, this failed to occur at E18.5 and their postnatal BAT could only sustain coupled respiration, indicating a perinatal requirement for IL-33 in licensing of thermogenesis. A similar defect in UCP1 protein expression was observed in P0.5 BAT of $Il1rl1^{-/-}$ mice (Figure 7B), indicating perinatal requirement for ST2 in licensing of uncoupled respiration.

Using P0.5 BAT, we next examined the relationship between UCP1 protein deficiency and the onset of mitochondrial dysfunction. We found that although P0.5 BAT of $Il33^{-/-}$, $Il1rl1^{-/-}$, and $Ucp1^{-/-}$ mice lacked UCP1 protein (Figure 7A, B and data not shown), the expression of respiratory chain components was unaffected (Figure 7C). In agreement with this, the activity of complex IV was not significantly different amongst the genotypes, whereas complex I activity was modestly reduced (~7%) in P0.5 BAT of $Ucp1^{-/-}$ mice (Figure 7D, E). Transmission electron microscopy confirmed that the ultrastructural changes observed in mitochondria of ~5-week-old $Il33^{-/-}$ and ~4-week-old $Ucp1^{-/-}$ mice were absent in P0.5 BAT (Figure 7F-H). In aggregate, these data suggest that UCP1 deficiency

precedes the onset of mitochondrial dysfunction observed in older *Il33*⁻/⁻ or *Ucp1*⁻/⁻ mice, and *Ucp1* is likely the primary target of IL-33 for perinatal licensing of uncoupled respiration in thermogenic adipocytes.

DISCUSSION

It is well-appreciated that UCP1-mediated uncoupled respiration is critical for thermogenesis and the maintenance of core temperature in adult animals (Bachman et al., 2002; Enerback et al., 1997). While the regulation of UCP1 is well-studied in adult animals, it is not known how UCP1 expression and activity are controlled during the perinatal period when developing embryos undergo their one-way transition to postnatal life. Here, we provide evidence for a surprising requirement for IL-33 and its receptor ST2 in perinatal licensing of uncoupled respiration in thermogenic adipocytes. Our data indicate that the IL-33:ST2 axis regulates the splicing of *Ucp1* mRNA during the perinatal period to ensure UCP1-mediated uncoupled respiration is activated in BAT just prior to birth. In the absence of IL-33 or ST2, beige and brown adipocytes develop normally, but can only support coupled respiration. While this is sufficient for adaptation of mutant mice to mild thermal stress (such as at 22°C, a temperature below their thermoneutral zone), they rapidly become hypothermic during a severe cold challenge (at 4-5°C), traits that phenocopy *Ucp1*⁻/⁻ mice.

Multiple lines of evidence suggest that *Ucp1* is likely the primary target of IL-33 in licensing of uncoupled respiration in thermogenic adipocytes. For example, we find that deficiency of IL-33 or ST2 does not affect the development and differentiation of beige or brown adipocytes. This was confirmed by genome-wide analysis of beige and brown adipose tissue from *Il33*⁻/⁻ mice animals, showing that expression of tissue-specific and thermogenic programs was unaffected. Furthermore, even the respiratory and ultrastructural defects observed in mitochondria of *Il33*⁻/⁻ BAT are likely to be secondary to UCP1 deficiency, because they were absent in neonatal (P0.5) BAT of *Il33*⁻/⁻ mice, which lack UCP1. Genetic support for this hypothesis was obtained from BAT of *Ucp1*⁻/⁻ mice, which exhibit a similar temporal pattern of respiratory and ultrastructural defects in their mitochondria, indicating that deficiency of UCP1 is sufficient to promote mitochondrial dysfunction as animals age.

Our findings suggest that IL-33:ST2 function as a developmental switch to control the splicing of functional *Ucp1* mRNAs in beige and brown adipocytes. Although we initially uncovered the presence of alternatively spliced forms of *Ucp1* mRNA in *Il33*-deficient BAT, additional analyses of embryonic and postnatal BAT revealed that they were also present in WT mice. Moreover, since the presence or absence of IL-33 or ST2 altered the ratio between normal (A) and alternatively spliced variant (C) of *Ucp1* in an almost all-or-none manner, it suggests that IL-33:ST2 axis functions as a binary switch to control the amount of functional UCP1 that is expressed in thermogenic adipocytes. Our inability to detect splice variant B, which utilizes a more proximal splice acceptor site and lacks only 9 amino acids, in beige or brown adipocytes of WT mice, potentially points to its generation as a compensatory response to the absence of functional UCP1 protein in *Il33*⁻/⁻ mice.

A key question that emerges from our work is how does IL-33 regulate splicing and expression of UCP1 in thermogenic adipocytes. Although elucidation of the precise

mechanism awaits further study, our data suggest that it is unlikely to be the canonical pathway by which IL-33 signals in immune cells. First, unlike in immune cells where there is epistasis between IL-33, ST2, and MyD88, we find that the downstream adaptor protein MyD88 is dispensable for licensing of uncoupled respiration in brown and beige adipocytes. Second, Tregs and ILC2s, two cell types responsive to IL-33 in adipose depots (Bapat et al., 2015; Kolodin et al., 2015; Molofsky et al., 2013; Vasanthakumar et al., 2015), are not required for licensing of BAT, because RRDD (lacking ILC2s) and Rag2$^{-/-}$γc$^{-/-}$ mice (lacking all adaptive immune cells and ILCs) have normal expression of UCP1 protein. Third, we observe that IL-33 is required for normal splicing of *Ucp1* mRNA in BAT, a function that is distinct from the gene expression programs it regulates in ILC2s and Tregs. Fourth, administration of recombinant cleaved IL-33, which signals via ST2 and MyD88 in immune cells, fails to rescue the respiratory defects in BAT of adult *Il33*$^{-/-}$ mice. While these results potentially point to a nuclear function of this atypical cytokine, a better understanding of its developmental pattern of expression, cleavage, release, and signaling will be necessary to elucidate the underlying mechanisms by which IL-33 regulates splicing of *Ucp1* mRNA.

While our data have uncovered an unexpected role for IL-33 in perinatal licensing of uncoupled respiration in brown adipocytes, its timing, sources and targets remain unclear for now. For example, we found that *Il33*$^{-/-}$ BAT fails to express UCP1 protein at E18.5, suggesting that IL-33 is likely to be required at some point prior to E18.5. During this developmental period, there are two potential sources of IL-33: the embryo and the mother, and two cellular targets for its action: in brown adipocyte precursors and differentiated brown adipocytes. Thus, in the future, it will be important to identify the cell types that express IL-33 during the perinatal period and examine whether its release is constitutive, timed for delivery, or induced by environmental cold. In addition, generation of cell- and tissue-specific knockouts of IL-33 and ST2 will be necessary to pinpoint the critical cell types that release IL-33 and the targets on which it acts to perinatally license thermogenesis, respectively.

In addition to regulation of thermogenesis, our findings have broader implications for how organogenesis is regulated in placental mammals. Unlike other metazoans, placental mammals face an additional hurdle during their development: the rapid transition from the intrauterine environment of the mother to the extrauterine environment in which they will spend the remainder of their lives. This brief perinatal period (from late embryogenesis to early postnatal life) is the critical time window during which many mammalian organs, such as liver, lungs, and brown adipose tissue, undergo essential maturation necessary for adaptation to postnatal life. For example, preterm infants are susceptible to hypoglycemia, hypoxia, and hypothermia due to impairment in liver (glucose production), lung (air exchange), and brown adipose tissue (heat production) function (Raju, 2012). Moreover, if the timing of this transition is not precisely correct, organs become susceptible to end organ damage, as demonstrated by the development of necrotizing colitis and respiratory distress syndrome in preterm infants (Raju, 2012). Despite its importance, how placental mammals regulate the perinatal maturation of their organs to prepare for the challenges of postnatal life has remained poorly understood.

Using BAT as model system, our work suggests that licensing of postnatal functions in placental organs is signal-dependent and independent of tissue differentiation programs. These findings lead us to propose a model in which three distinct classes of signals regulate organogenesis in placental mammals. While developmental signals (BMPs, Wnts, Hedgehogs, FGFs, and Notch ligands) and their downstream transcription factors regulate cellular programs of patterning, differentiation, and tissue growth during early embryogenesis, the neuroendocrine and immune systems regulate the physiological responsiveness of these tissues to maintain homeostasis in the adult. Our studies suggest that IL-33 is an example of and belongs to a previously unappreciated group of perinatal signals, which function as a developmental switch to license and prepare tissues for postnatal life. In this context, it is intriguing to note *Il1rl1* (encoding ST2) and *MyD88* are evolutionarily ancient (found in fish, reptiles, birds, and all infraclasses of mammals) (Sattler et al., 2013), whereas *Il33* is only present in the placental mammals but not in monotremes and marsupials, the two infraclasses of mammals that do not have a need for perinatal licensing of thermogenesis because they are egg-laying or complete their development in a warm external pouch.

EXPERIMENTAL PROCEDURES

Animal studies

All animal studies were conducted under an approved IACUC protocol at UCSF. All animals were congenic to the C57BL6/J background and housed at 22°C (unless otherwise indicated) in the vivarium under a 12 hour light:dark cycle. Both male and female mice of various ages were used in these studies. C57BL/6J mice were purchased from Jackson Laboratories and bred in our vivarium; *Il33*$^{-/-}$ were kindly provided by Jean-Philippe Girard via Richard Locksley (Pichery et al., 2012), *Il1rl1*$^{-/-}$ were kindly provided by Shizuo Akira via Richard Locksley (Hoshino et al., 1999), RR and RRDD mice were kindly provided by Richard Locksley, and *Ucp1*$^{-/-}$ were kindly provided by Lesley Kozak via Yuriy Kirichok (Enerback et al., 1997). The cold exposure experiments were performed as described previously (Lee et al., 2015). Mouse core (rectal) temperature was measured hourly using a BAT-12 microprobe thermometer with RET-3 thermocouple (PhysiTemp). As per IACUC guidelines, "survival" was defined as a core temperature >28°C. For cohousing experiments, WT and *Il33*$^{-/-}$ litters were swapped between dams at P0.5. For rescue experiments, 6 week-old mice were injected intraperitoneally with vehicle, IL-33 (0.5 g, Biolegend), CL-316,243 (1 mg/kg, Sigma) or both daily for 1 week. For all *in vivo* studies, cohorts of 4 mice per genotype or treatment were assembled, and experiments were repeated 2-3 independent times.

Statistical analysis

Data were analyzed using Prism (Graphpad) and are presented as mean ± s.e.m. Statistical significance was determined using the unpaired two-tailed Student's t-test for single variables and two-way ANOVA followed by Bonferroni post-tests for multiple variables. For survival experiments, statistical significance was determined using the Mantel-Cox log-rank test. A p-value of < 0.05 was considered to be statistically significant and is presented as * ($p < 0.05$), ** ($p < 0.01$), or *** ($p < 0.001$).

Supplementary Material

Refer to Web version on PubMed Central for supplementary material.

REFERENCES

Azzu V, Brand MD. The on-off switches of the mitochondrial uncoupling proteins. Trends Biochem Sci. 2010; 35:298–307. [PubMed: 20006514]

Bachman ES, Dhillon H, Zhang CY, Cinti S, Bianco AC, Kobilka BK, Lowell BB. betaAR signaling required for diet-induced thermogenesis and obesity resistance. Science. 2002; 297:843–845. [PubMed: 12161655]

Bapat SP, Myoung Suh J, Fang S, Liu S, Zhang Y, Cheng A, Zhou C, Liang Y, LeBlanc M, Liddle C, et al. Depletion of fat-resident Treg cells prevents age-associated insulin resistance. Nature. 2015; 528:137–141. [PubMed: 26580014]

Berriz GF, King OD, Bryant B, Sander C, Roth FP. Characterizing gene sets with FuncAssociate. Bioinformatics. 2003; 19:2502–2504. [PubMed: 14668247]

Brestoff JR, Kim BS, Saenz SA, Stine RR, Monticelli LA, Sonnenberg GF, Thome JJ, Farber DL, Lutfy K, Seale P, et al. Group 2 innate lymphoid cells promote beiging of white adipose tissue and limit obesity. Nature. 2015; 519:242–246. [PubMed: 25533952]

Cannon B, Nedergaard J. Nonshivering thermogenesis and its adequate measurement in metabolic studies. The Journal of experimental biology. 2011; 214:242–253. [PubMed: 21177944]

Cayrol C, Girard JP. IL-33: an alarmin cytokine with crucial roles in innate immunity, inflammation and allergy. Current opinion in immunology. 2014; 31C:31–37. [PubMed: 25278425]

Chen WY, Hong J, Gannon J, Kakkar R, Lee RT. Myocardial pressure overload induces systemic inflammation through endothelial cell IL-33. Proc Natl Acad Sci U S A. 2015; 112:7249–7254. [PubMed: 25941360]

Cohen P, Spiegelman BM. Brown and Beige Fat: Molecular Parts of a Thermogenic Machine. Diabetes. 2015; 64:2346–2351. [PubMed: 26050670]

Enerback S, Jacobsson A, Simpson EM, Guerra C, Yamashita H, Harper ME, Kozak LP. Mice lacking mitochondrial uncoupling protein are cold-sensitive but not obese. Nature. 1997; 387:90–94. [PubMed: 9139827]

Fedorenko A, Lishko PV, Kirichok Y. Mechanism of fatty-acid-dependent UCP1 uncoupling in brown fat mitochondria. Cell. 2012; 151:400–413. [PubMed: 23063128]

Feldmann HM, Golozoubova V, Cannon B, Nedergaard J. UCP1 ablation induces obesity and abolishes diet-induced thermogenesis in mice exempt from thermal stress by living at thermoneutrality. Cell Metab. 2009; 9:203–209. [PubMed: 19187776]

Frontini A, Cinti S. Distribution and development of brown adipocytes in the murine and human adipose organ. Cell Metab. 2010; 11:253–256. [PubMed: 20374956]

Golozoubova V, Hohtola E, Matthias A, Jacobsson A, Cannon B, Nedergaard J. Only UCP1 can mediate adaptive nonshivering thermogenesis in the cold. FASEB journal : official publication of the Federation of American Societies for Experimental Biology. 2001; 15:2048–2050. [PubMed: 11511509]

Gordon, CJ. Temperature regulation in laboratory rodents. Cambridge University Press; Cambridge England ; New York, NY, USA: 1993.

Harms M, Seale P. Brown and beige fat: development, function and therapeutic potential. Nat Med. 2013; 19:1252–1263. [PubMed: 24100998]

Hofmann WE, Liu X, Bearden CM, Harper ME, Kozak LP. Effects of genetic background on thermoregulation and fatty acid-induced uncoupling of mitochondria in UCP1-deficient mice. J Biol Chem. 2001; 276:12460–12465. [PubMed: 11279075]

Hoshino K, Kashiwamura S, Kuribayashi K, Kodama T, Tsujimura T, Nakanishi K, Matsuyama T, Takeda K, Akira S. The absence of interleukin 1 receptor-related T1/ST2 does not affect T helper cell type 2 development and its effector function. The Journal of experimental medicine. 1999; 190:1541–1548. [PubMed: 10562328]

Karp CL. Unstressing intemperate models: how cold stress undermines mouse modeling. The Journal of experimental medicine. 2012; 209:1069–1074. [PubMed: 22665703]

Kazak L, Chouchani ET, Jedrychowski MP, Erickson BK, Shinoda K, Cohen P, Vetrivelan R, Lu GZ, Laznik-Bogoslavski D, Hasenfuss SC, et al. A creatine-driven substrate cycle enhances energy expenditure and thermogenesis in beige fat. Cell. 2015; 163:643–655. [PubMed: 26496606]

Klingenberg M, Echtay KS, Bienengraeber M, Winkler E, Huang SG. Structure-function relationship in UCP1. Int J Obes Relat Metab Disord. 1999; 23(Suppl 6):S24–29. [PubMed: 10454117]

Kolodin D, van Panhuys N, Li C, Magnuson AM, Cipolletta D, Miller CM, Wagers A, Germain RN, Benoist C, Mathis D. Antigen- and cytokine-driven accumulation of regulatory T cells in visceral adipose tissue of lean mice. Cell Metab. 2015; 21:543–557. [PubMed: 25863247]

Lee MW, Odegaard JI, Mukundan L, Qiu Y, Molofsky AB, Nussbaum JC, Yun K, Locksley RM, Chawla A. Activated type 2 innate lymphoid cells regulate beige fat biogenesis. Cell. 2015; 160:74–87. [PubMed: 25543153]

Liu X, Rossmeisl M, McClaine J, Riachi M, Harper ME, Kozak LP. Paradoxical resistance to diet-induced obesity in UCP1-deficient mice. J Clin Invest. 2003; 111:399–407. [PubMed: 12569166]

Lowell BB, Spiegelman BM. Towards a molecular understanding of adaptive thermogenesis. Nature. 2000; 404:652–660. [PubMed: 10766252]

Molofsky AB, Nussbaum JC, Liang HE, Van Dyken SJ, Cheng LE, Mohapatra A, Chawla A, Locksley RM. Innate lymphoid type 2 cells sustain visceral adipose tissue eosinophils and alternatively activated macrophages. The Journal of experimental medicine. 2013; 210:535–549. [PubMed: 23420878]

Molofsky AB, Savage AK, Locksley RM. Interleukin-33 in Tissue Homeostasis, Injury, and Inflammation. Immunity. 2015; 42:1005–1019. [PubMed: 26084021]

Moro K, Yamada T, Tanabe M, Takeuchi T, Ikawa T, Kawamoto H, Furusawa J, Ohtani M, Fujii H, Koyasu S. Innate production of T(H)2 cytokines by adipose tissue-associated c-Kit(+)Sca-1(+) lymphoid cells. Nature. 2010; 463:540–544. [PubMed: 20023630]

Neill DR, Wong SH, Bellosi A, Flynn RJ, Daly M, Langford TK, Bucks C, Kane CM, Fallon PG, Pannell R, et al. Nuocytes represent a new innate effector leukocyte that mediates type-2 immunity. Nature. 2010; 464:1367–1370. [PubMed: 20200518]

Nguyen KD, Fentress SJ, Qiu Y, Yun K, Cox JS, Chawla A. Circadian gene Bmal1 regulates diurnal oscillations of Ly6C(hi) inflammatory monocytes. Science. 2013; 341:1483–1488. [PubMed: 23970558]

Nussbaum JC, Van Dyken SJ, von Moltke J, Cheng LE, Mohapatra A, Molofsky AB, Thornton EE, Krummel MF, Chawla A, Liang HE, et al. Type 2 innate lymphoid cells control eosinophil homeostasis. Nature. 2013; 502:245–248. [PubMed: 24037376]

Pichery M, Mirey E, Mercier P, Lefrancais E, Dujardin A, Ortega N, Girard JP. Endogenous IL-33 is highly expressed in mouse epithelial barrier tissues, lymphoid organs, brain, embryos, and inflamed tissues: in situ analysis using a novel Il-33-LacZ gene trap reporter strain. J Immunol. 2012; 188:3488–3495. [PubMed: 22371395]

Price AE, Liang HE, Sullivan BM, Reinhardt RL, Eisley CJ, Erle DJ, Locksley RM. Systemically dispersed innate IL-13-expressing cells in type 2 immunity. Proc Natl Acad Sci U S A. 2010; 107:11489–11494. [PubMed: 20534524]

Qiu Y, Nguyen KD, Odegaard JI, Cui X, Tian X, Locksley RM, Palmiter RD, Chawla A. Eosinophils and type 2 cytokine signaling in macrophages orchestrate development of functional beige fat. Cell. 2014; 157:1292–1308. [PubMed: 24906148]

Raju TN. Developmental physiology of late and moderate prematurity. Semin Fetal Neonatal Med. 2012; 17:126–131. [PubMed: 22317884]

Rao RR, Long JZ, White JP, Svensson KJ, Lou J, Lokurkar I, Jedrychowski MP, Ruas JL, Wrann CD, Lo JC, et al. Meteorin-like Is a Hormone that Regulates Immune-Adipose Interactions to Increase Beige Fat Thermogenesis. Cell. 2014; 157:1279–1291. [PubMed: 24906147]

Sattler S, Smits HH, Xu D, Huang FP. The evolutionary role of the IL-33/ST2 system in host immune defence. Arch Immunol Ther Exp (Warsz). 2013; 61:107–117. [PubMed: 23283516]

Schmitz J, Owyang A, Oldham E, Song Y, Murphy E, McClanahan TK, Zurawski G, Moshrefi M, Qin J, Li X, et al. IL-33, an interleukin-1-like cytokine that signals via the IL-1 receptor-related protein ST2 and induces T helper type 2-associated cytokines. Immunity. 2005; 23:479–490. [PubMed: 16286016]

Sidossis L, Kajimura S. Brown and beige fat in humans: thermogenic adipocytes that control energy and glucose homeostasis. J Clin Invest. 2015; 125:478–486. [PubMed: 25642708]

Tian XY, Ganeshan K, Hong C, Nguyen KD, Qiu Y, Kim J, Tangirala RK, Tonotonoz P, Chawla A. Thermoneutral Housing Accelerates Metabolic Inflammation to Potentiate Atherosclerosis but Not Insulin Resistance. Cell Metab. 2016; 23:165–178. [PubMed: 26549485]

Ukropec J, Anunciado RP, Ravussin Y, Hulver MW, Kozak LP. UCP1-independent thermogenesis in white adipose tissue of cold-acclimated Ucp1−/− mice. J Biol Chem. 2006; 281:31894–31908. [PubMed: 16914547]

Van Dyken SJ, Mohapatra A, Nussbaum JC, Molofsky AB, Thornton EE, Ziegler SF, McKenzie AN, Krummel MF, Liang HE, Locksley RM. Chitin activates parallel immune modules that direct distinct inflammatory responses via innate lymphoid type 2 and gammadelta T cells. Immunity. 2014; 40:414–424. [PubMed: 24631157]

Vasanthakumar A, Moro K, Xin A, Liao Y, Gloury R, Kawamoto S, Fagarasan S, Mielke LA, Afshar-Sterle S, Masters SL, et al. The transcriptional regulators IRF4, BATF and IL-33 orchestrate development and maintenance of adipose tissue-resident regulatory T cells. Nat Immunol. 2015; 16:276–285. [PubMed: 25599561]

Vosselman MJ, van Marken Lichtenbelt WD, Schrauwen P. Energy dissipation in brown adipose tissue: from mice to men. Molecular and cellular endocrinology. 2013; 379:43–50. [PubMed: 23632102]

Xue B, Rim JS, Hogan JC, Coulter AA, Koza RA, Kozak LP. Genetic variability affects the development of brown adipocytes in white fat but not in interscapular brown fat. Journal of lipid research. 2007; 48:41–51. [PubMed: 17041251]

HIGHLIGHTS

- IL-33 and ST2 license uncoupled respiration in beige and brown adipocytes

- Genetic absence of IL-33 or ST2 impairs adaptation to environmental cold

- IL-33 and ST2 regulate splicing of Ucp1 mRNA in thermogenic adipocytes

- Perinatal licensing of brown adipocytes for uncoupled respiration requires IL-33
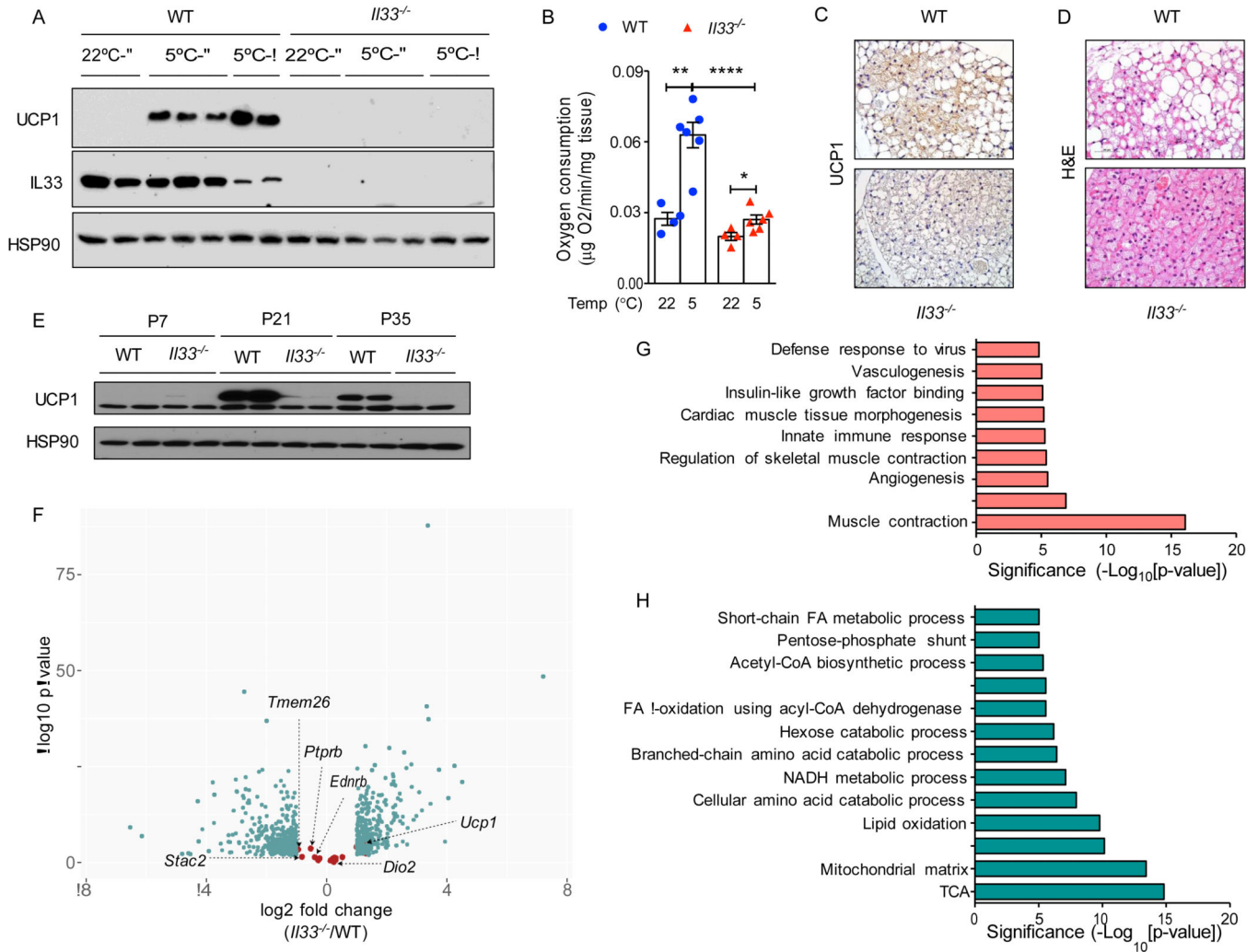
Figure 1. IL-33 is required for uncoupled respiration in beige adipocytes
(A) Immunoblotting for UCP1 in iWAT of WT and *Il33⁻/⁻* male and female mice housed at 22°C or 5°C for 48 hours (n=2-3 per temperature and gender). (B) Ex vivo oxygen consumption rate in iWAT of WT and *Il33⁻/⁻* mice housed at 22°C or 5°C for 48 hours (n=4-6 per genotype and temperature). (C, D) Representative sections of iWAT from WT and *Il33⁻/⁻* mice housed at 5°C for 48 hours were stained for UCP1 (C) or with hematoxylin and eosin, 400x magnification. (E) Immunoblotting for UCP1 in iWAT of WT and *Il33⁻/⁻* mice housed at 22°C (n=2 per gender and age). (F) RNA-seq analysis of iWAT at P24 from WT and *Il33⁻/⁻* mice housed at 22°C. Volcano plot displaying fold change (log2) of mRNA expression is shown. Beige fat markers are highlighted in salmon, whereas differentially expressed mRNAs (FDR<5% and >2-fold expression) are shown in teal (n=3-4 per genotype). (G, H) Pathway analysis of a subset of mRNAs suppressed (G) or induced (H) >2-fold in P24 iWAT of WT and *Il33⁻/⁻* mice housed at 22°C (n=3-4 per genotype). Data are represented as mean ± SEM. See also Figure S1 and Tables S1-S3.
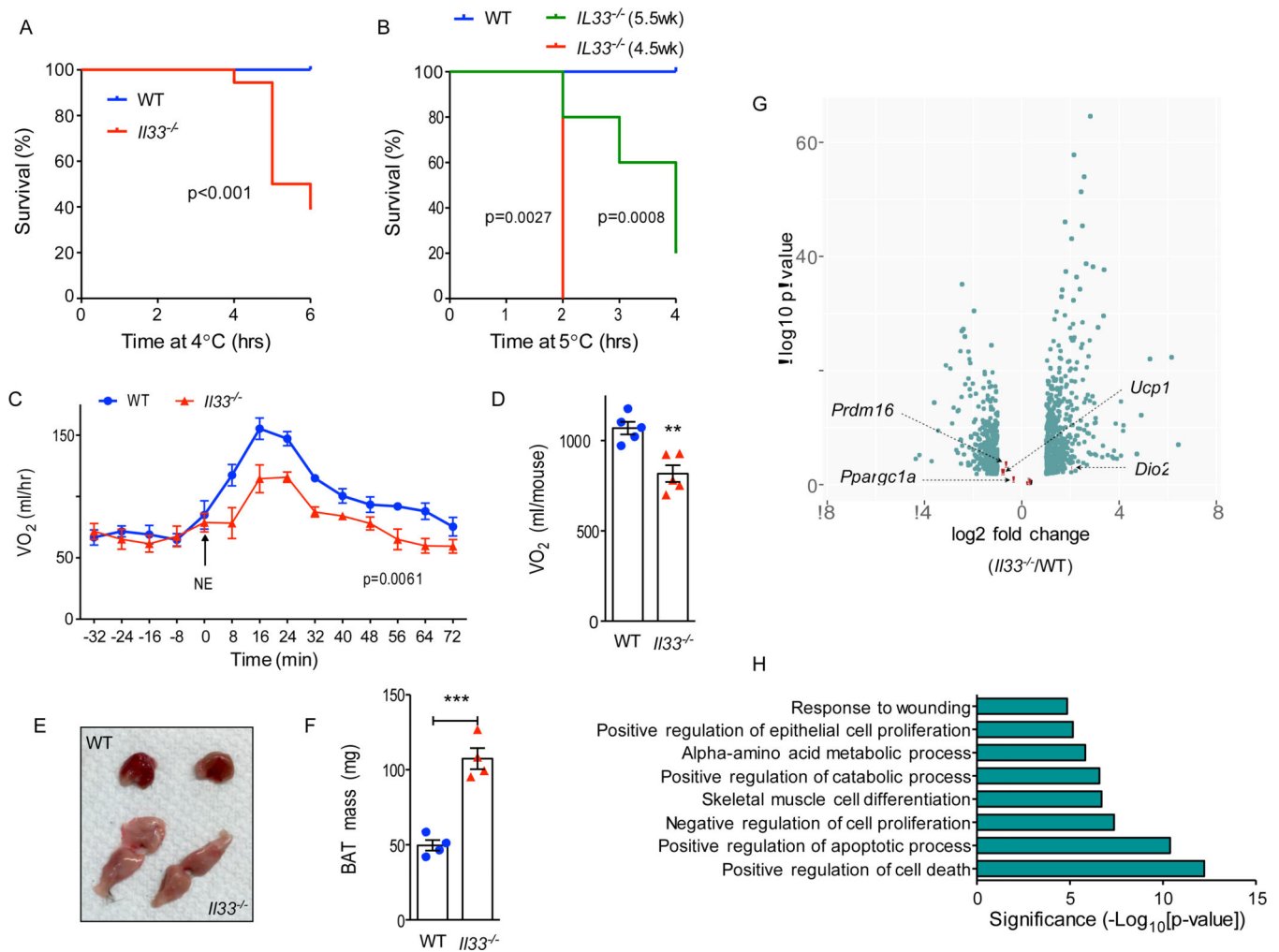
Figure 2. Defective cold-induced thermogenesis in *Il33*⁻/⁻ mice

(A, B) Survival curves of WT and *Il33*⁻/⁻ mice challenged with environmental cold (4-5°C). Mice were euthanized when their core temperature was 28°C. (A) Survival curves for 8-10-week-old male and female mice (n=9-10 per genotype). (B) Survival curves for 4.5- and 5.5-week-old male and female WT and *Il33*⁻/⁻ mice (n=5-10 per genotype). (C, D) Norepinephrine stimulated changes in oxygen consumption (VO) in conscious WT and *Il33*⁻/⁻ mice housed at 22°C (n=5 per genotype). (E, F) Representative gross histology (E) and mass (F) of BAT from ~6-week-old-female WT and *Il33*⁻/⁻ mice housed 22°C (n=4 per genotype). (G) RNA-seq analysis of BAT at P0.5 from WT and *Il33*⁻/⁻ mice housed at 22°C. Volcano plot displaying fold change (log2) of mRNA expression is shown. Brown fat markers are highlighted in salmon, whereas differentially expressed mRNAs (FDR<5% and >2-fold expression) are shown in teal (n=4 per genotype). (H) Pathway analysis of a subset of mRNAs induced >2-fold in P0.5 BAT of WT and *Il33*⁻/⁻ mice housed at 22°C (n=4 per genotype). Data are represented as mean ± SEM. See also Figure S1 and Tables S4, S5.
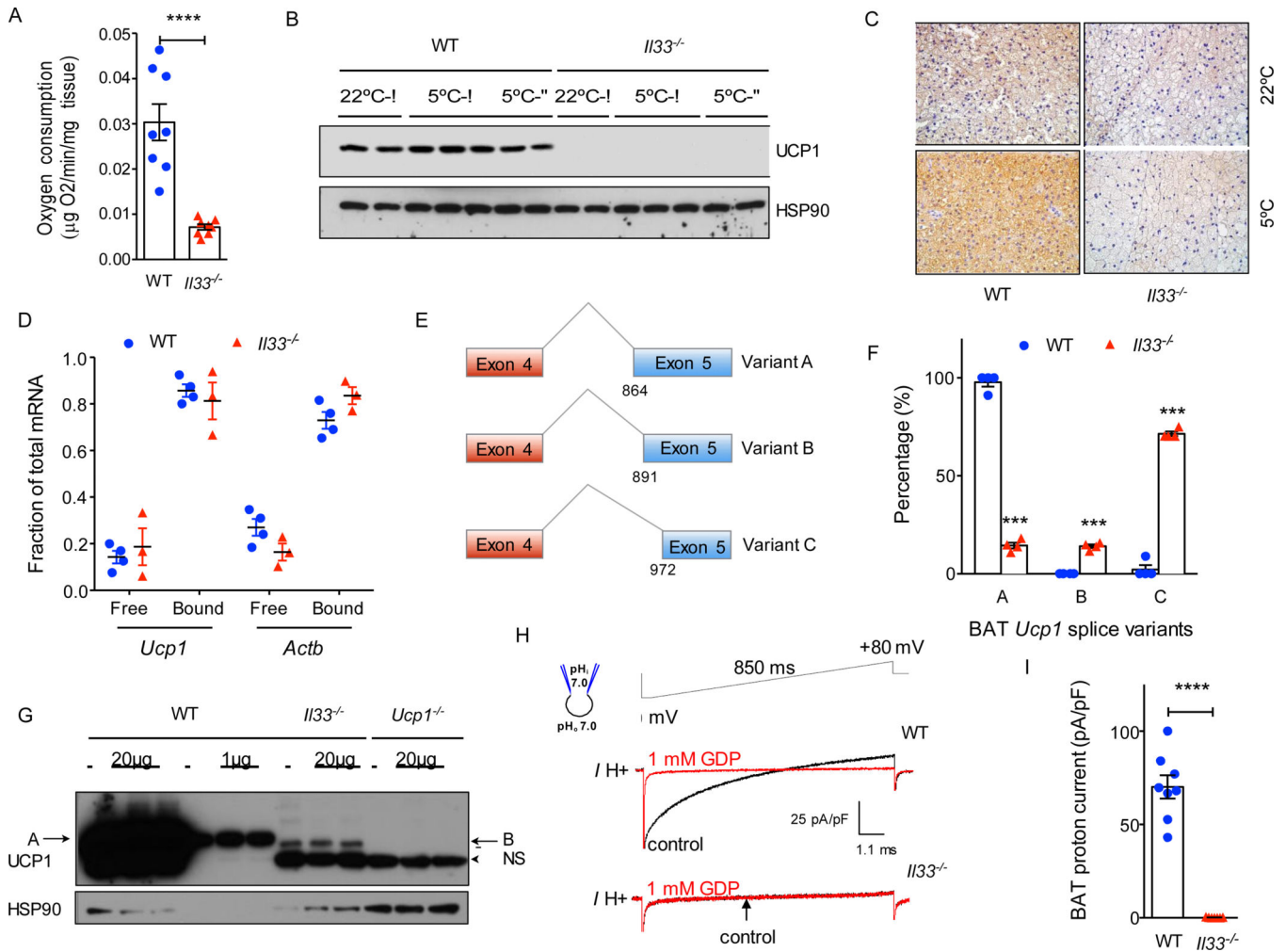
Figure 3. IL-33 is required for splicing of Ucp1 mRNA and expression of functional UCP1
(A) Oxygen consumption rate in BAT of WT and *Il33−/−* mice housed at 22°C (n=8 per
genotype). (B) Immunoblotting for UCP1 protein in BAT of WT and *Il33−/−* male and
female mice housed at 22°C or 5°C (n=2-3 per temperature and gender). (C)
Immunostaining for UCP1 in representative sections of BAT from WT and *Il33−/−* mice
housed at 22°C or 5°C. (D) Polysome analysis. (E) Schematic diagram showing alternative
splice variants generated from activation of cryptic splice acceptor sites in exon 5 of *Ucp1*.
Variant A utilizes the normal splice junctions between exons 4 and 5, whereas variants B and
C use cryptic splice sites in exon 5. (F) Quantification of *Ucp1* splice variants present in
BAT of P0.5 WT and *Il33−/−* mice. Analysis of *Ucp1* mRNA splicing was performed using
the RNA-seq datasets. (G) Immunoblotting for UCP1 in BAT of WT, *Il33−/−* and
Ucp1−/− 0.5 day-old mice (n=3 per genotype); NS-non-specific, A-variant A, B-variant B.
(H) Representative currents recorded in whole-mitoplasts prepared from WT and *Il33−/−*
BAT. Whole-mitoplast UCP1 current before (black) and after (red) addition of 1 mM GDP to
the bath solution. The voltage protocol is indicated at the top. The pipette-mitoplast diagram
indicates the recording conditions. (I) Quantification of UCP1 current in whole-mitoplasts
prepared from WT and *Il33−/−* BAT (n=7-8 per genotype). See also Figures S2 and S3.
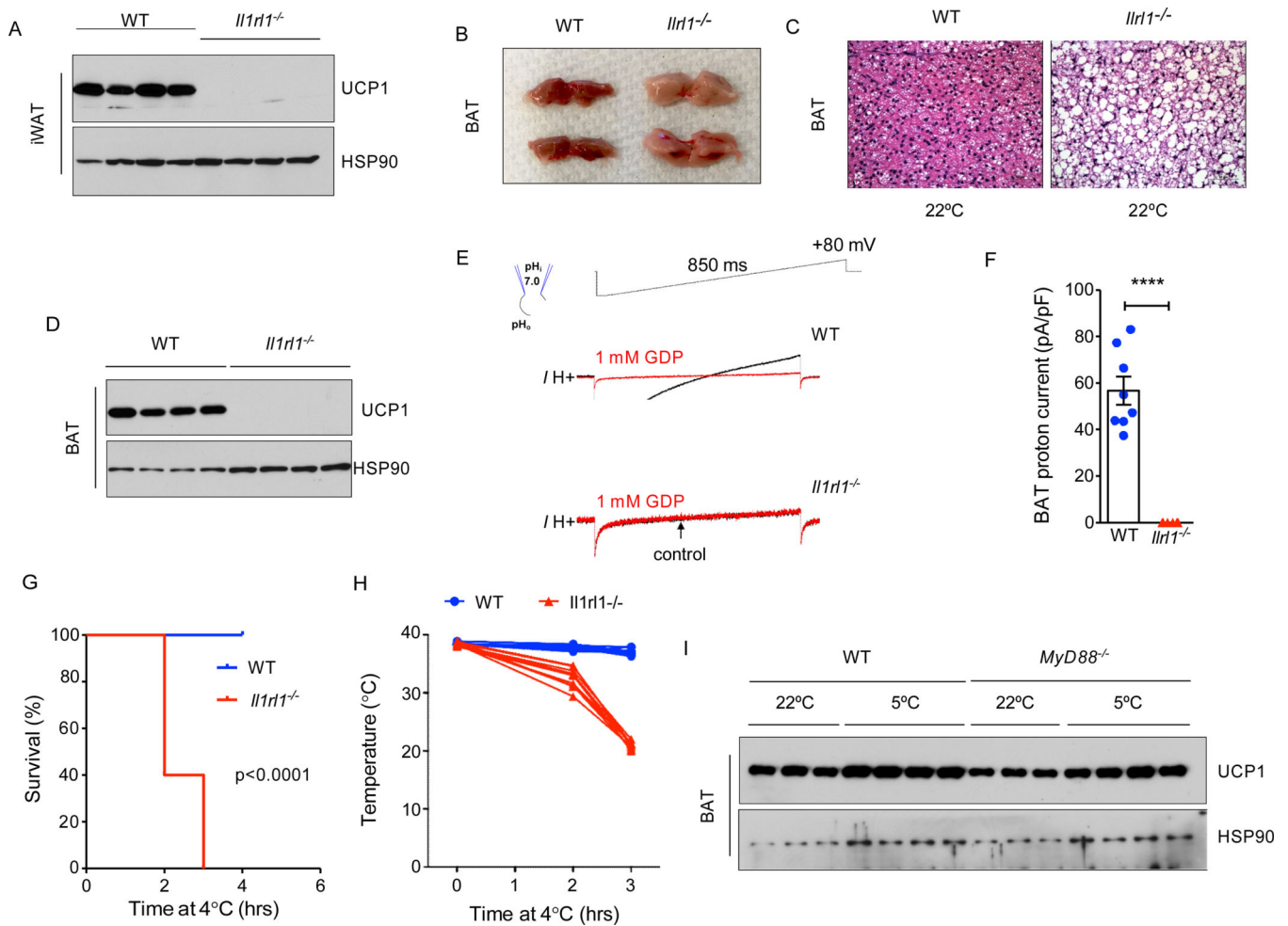
Figure 4. ST2 is required for uncoupled respiration in thermogenic adipocytes

(A) Immunoblotting for UCP1 in iWAT of WT and $Il1rl1^{-/-}$ 3-week-old mice housed at 22°C (n=4 per genotype). (B, C) Representative gross histology (B), and hematoxylin and eosin (C) staining of representative sections of BAT of ~3-week-old WT and $Il1rl1^{-/-}$ mice housed 22°C (n=4 per genotype). (D) Immunoblotting for UCP1 protein in BAT of 3-week-old WT and $Il1rl1^{-/-}$ mice housed at 22°C (n=4 per genotype). (E) Representative currents recorded in whole-mitoplasts isolated from WT and $Il1rl1^{-/-}$ BAT. Whole-mitoplast UCP1 current before (black) and after (red) addition of 1 mM GDP to the bath solution. The voltage protocol is indicated at the top. The pipette-mitoplast diagram indicates the recording conditions. (F) Quantification of UCP1 current in whole-mitoplasts isolated from WT and $Il1rl1^{-/-}$ BAT. (G, H) Survival curve (G) and core temperature (H) of 4.5-week-old WT and $Il1rl1^{-/-}$ mice challenged with environmental cold (4-5°C). Mice were euthanized when their core temperature was 28°C (n=10 per genotype). (I) Immunoblotting for UCP1 protein in BAT of 12-week-old WT and $Myd88^{-/-}$ mice housed at 22°C or 5°C (n=3-4 per temperature and gender). Data are represented as mean ± SEM. See also Figure S4.
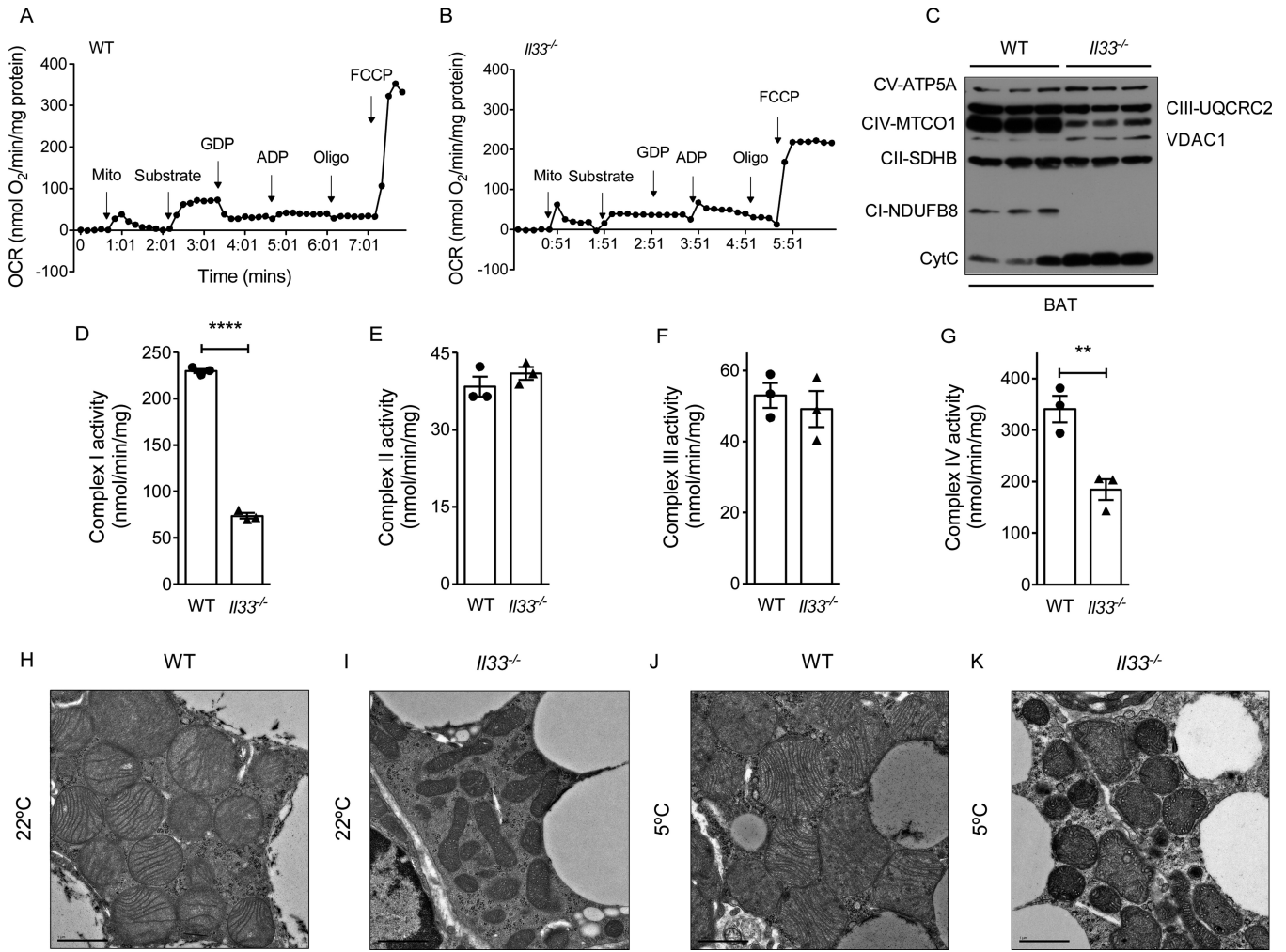
Figure 5. Reduced oxidative respiration and complex activity in mitochondria of IL-33 deficient BAT

(A, B) Representative recording of oxygen consumption by mitochondria purified from BAT of ~6-week-old WT and $Il33^{-/-}$ mice housed at 22°C (n=3-4 per genotype). (C) Immunoblotting for components of mitochondrial respiratory chain, VDAC1 and Cytochrome C in purified mitochondria from BAT of WT and $Il33^{-/-}$ mice housed at 22°C (n=3 per genotype). (D-G) Quantification of mitochondrial respiratory chain activities using mitochondria purified from BAT of ~6-week-old WT and $Il33^{-/-}$ mice housed at 22°C (n=3 per genotype). Complex I (D), complex II (E), complex III (F) and complex IV (G). (H-K) Representative transmission electron micrographs of BAT from ~5-week-old WT and $Il33^{-/-}$ mice housed at 22°C and 5°C, magnification 4000x. Data are represented as mean ± SEM. See also Figure S5.
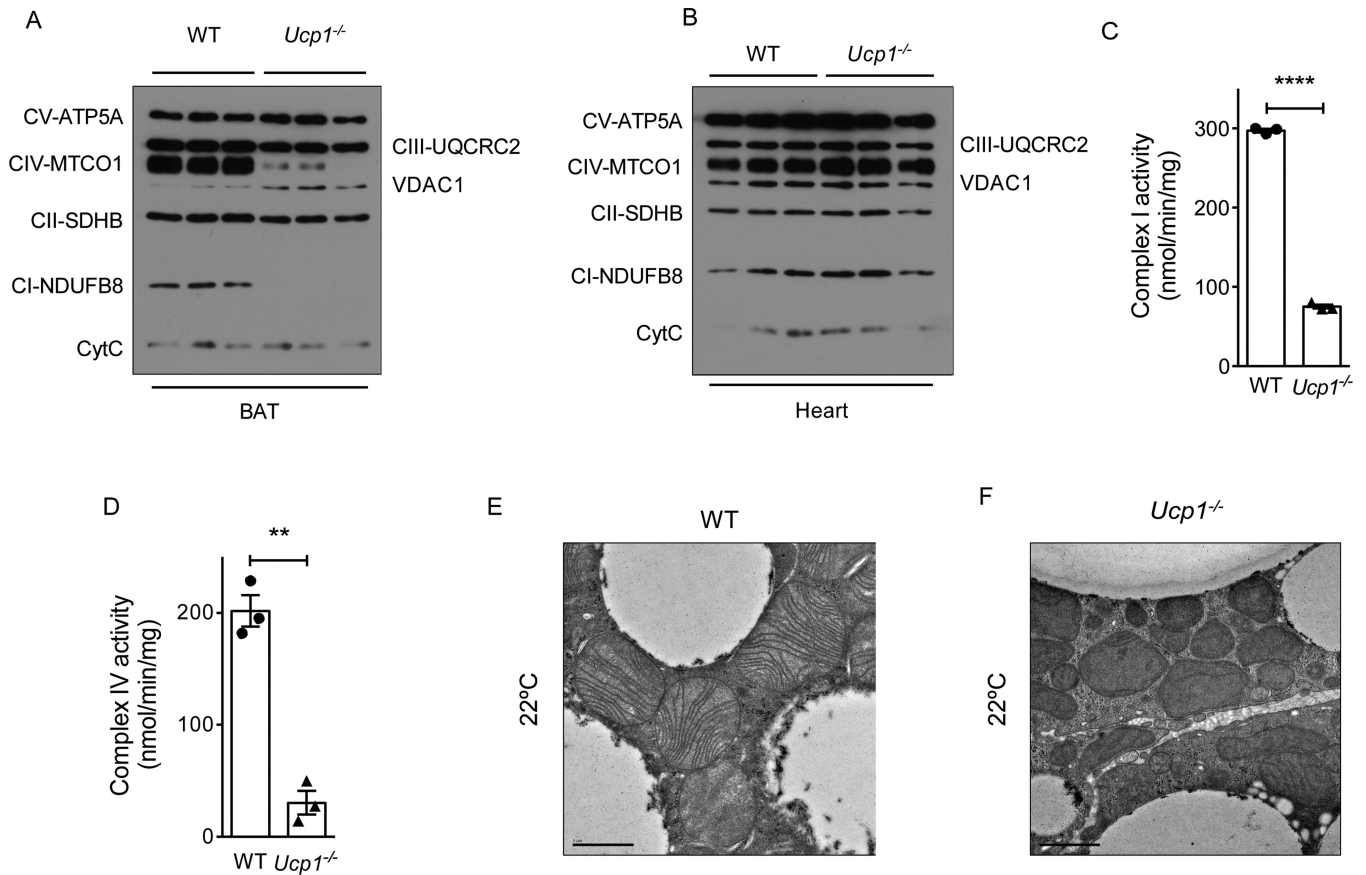
Figure 6. Mitochondria of *Ucp1*⁻/⁻ BAT have defects in respiratory complexes
(A, B) Immunoblotting for components of mitochondrial respiratory chain, VDAC1 and Cytochrome C in purified mitochondria from BAT (A) and heart (B) of ~6-week-old WT and *Ucp1*⁻/⁻ mice housed at 22°C (n=3 per genotype). (C, D) Quantification of complex I (C) and complex IV (D) activity in purified mitochondria from BAT of ~6-week-old WT and *Ucp1*⁻/⁻ mice housed at 22°C (n=3 per genotype). (E, F). Representative transmission electron micrographs of BAT from ~5-week-old WT and *Ucp1*⁻/⁻ mice housed at 22°C, magnification 4000x. Data are represented as mean ± SEM.
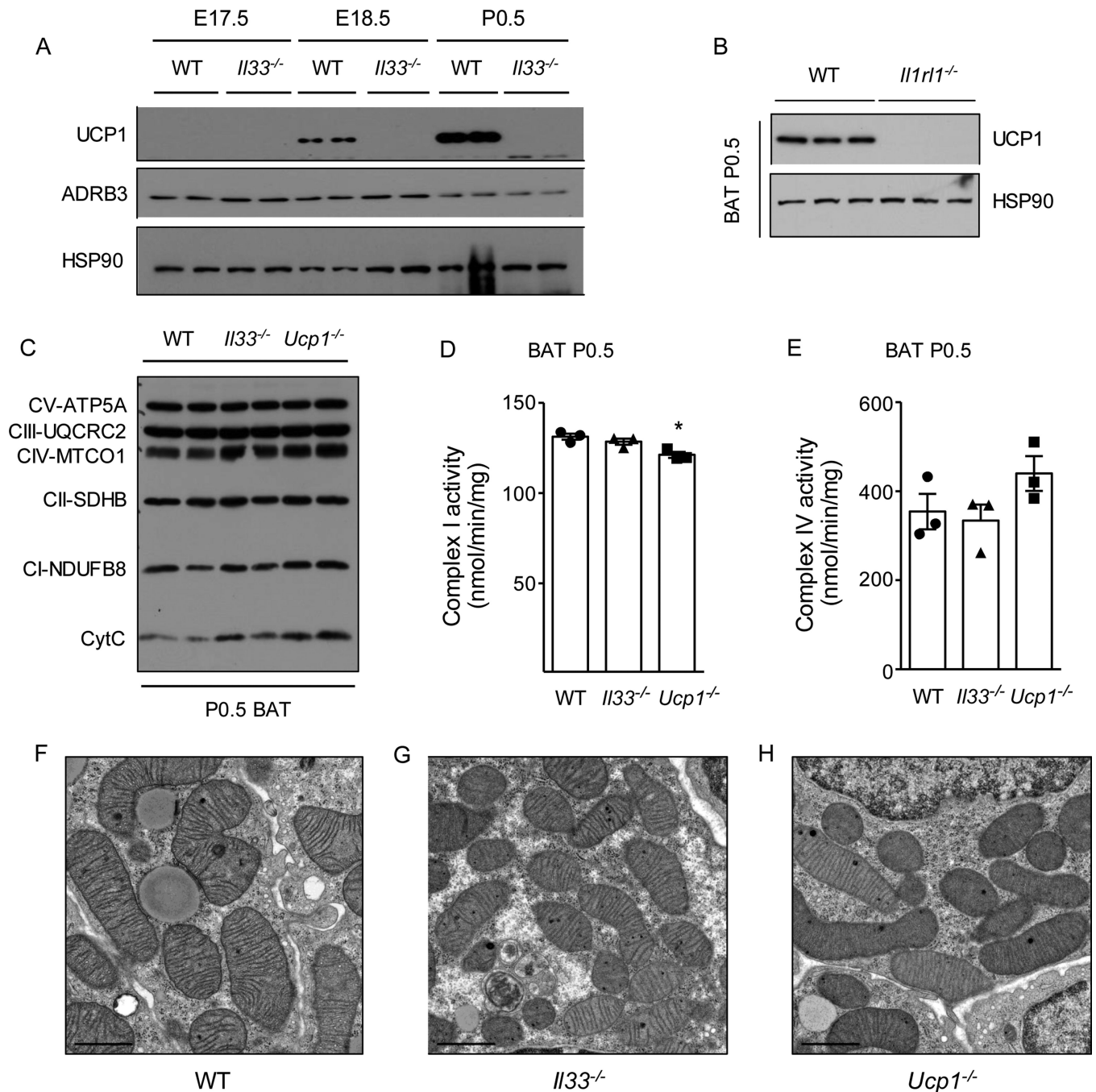
Figure 7. Perinatal requirement of IL-33 in licensing of uncoupled respiration

(A) Immunoblotting for UCP1 protein in BAT during the perinatal period in WT and *Il33⁻/⁻* mice housed at 22°C (n=2 per genotype and time point). (B) Immunoblotting for UCP1 protein in P0.5 BAT of WT and *Il1rl1⁻/⁻* mice housed at 22°C (n=3 per genotype). (C) Immunoblotting for components of mitochondrial respiratory chain and Cytochrome C in purified mitochondria from BAT of P0.5 WT, *Il33⁻/⁻*, and *Ucp1⁻/⁻* mice (n=2 per genotype). (D, E) Quantification of activities of complex I (D) and complex IV (E) in purified mitochondria from P0.5 BAT of WT, *Il33⁻/⁻*, and *Ucp1⁻/⁻* mice (n=3 per genotype). (F-H)

Representative transmission electron micrographs of P0.5 BAT of WT, *Il33*−/−, and *Ucp1*−/− mice, magnification 4000x. Data are represented as mean ± SEM.